



Damage analysis for thermal loading induced by laser impact in epoxy composite laminate

Cédric Huchette, Gillian Leplat, Valentin Biasi

► To cite this version:

Cédric Huchette, Gillian Leplat, Valentin Biasi. Damage analysis for thermal loading induced by laser impact in epoxy composite laminate. ECCM17, Jun 2016, MUNICH, Germany. hal-01414776

HAL Id: hal-01414776

<https://hal.science/hal-01414776>

Submitted on 12 Dec 2016

HAL is a multi-disciplinary open access archive for the deposit and dissemination of scientific research documents, whether they are published or not. The documents may come from teaching and research institutions in France or abroad, or from public or private research centers.

L'archive ouverte pluridisciplinaire **HAL**, est destinée au dépôt et à la diffusion de documents scientifiques de niveau recherche, publiés ou non, émanant des établissements d'enseignement et de recherche français ou étrangers, des laboratoires publics ou privés.

DAMAGE ANALYSIS FOR THERMAL LOADING INDUCED BY LASER IMPACT IN EPOXY COMPOSITE LAMINATE

Cédric Huchette¹, Gillian Leplat² and Valentin Biasi³

¹ DMSC, ONERA - The French Aerospace Lab - F-31055 Toulouse, France

Email: cedric.huchette@onera.fr, Web Page: <http://www.onera.fr>

² DMAE, UFT-MiP, ONERA - The French Aerospace Lab - F-31055 Toulouse, France

Email: gillian.leplat@onera.fr, Web Page: <http://www.onera.fr>

³ DMAE, UFT-MiP, ONERA - The French Aerospace Lab - F-31055 Toulouse, France

Email: valentin.biasi@onera.fr, Web Page: <http://www.onera.fr>

Keywords: fire, damage, delamination, thermal, modelling

Abstract

The thermal response of a composite material subjected to high heat flux is driven by heat conduction combined with endothermic (pyrolysis) and exothermic (oxidation) chemical reactions that change locally the thermo-physical properties and generate decomposition gas flowing throughout the porous charring medium. Heat and mass transfer is also affected by mechanical damage experienced by laminates such as matrix or interfacial cracking the origin of which may be related to internal stresses and thermal loads as well as pore and char formation. The challenge is to analyse concurrently the multi-physics phenomena in order to identify and understand the damage processes.

1. Introduction

The thermal response of a composite material subjected to high heat flux is driven by heat conduction combined with endothermic (pyrolysis) and exothermic (oxidation) chemical reactions that change locally the thermo-physical properties and generate decomposition gas flowing throughout the porous charring medium. Heat and mass transfer is also affected by mechanical damage experienced by laminates such as matrix or interfacial cracking the origin of which may be related to internal stresses and thermal loads as well as pore and char formation. The challenge is to analyse concurrently the multi-physics phenomena in order to identify and understand the damage processes.

However some progress has been made in understanding the composite thermo-mechanical behaviour when subjected to a fire [1-2], it remains the combination of complex interactions between the condensed phase and the gas phase within the material but also at the interface with the flame. It is all the more important since fire dynamics considerations are mandatory to assess relevant space and time distribution of the heat exchanges from the flame to the material surface. The conventional configurations and experimental setups [1-2] are designed to limit the analysis to the through-thickness direction while major composite laminates have an intrinsic orthotropic behaviour caused by the fibre reinforcement and the stacking sequence for laminates. The in-plane behaviour is unfortunately avoided while it may prevail in a practical event.

The present study is devoted to the analysis of the thermo-chemical phenomena and the induced damage occurring within decomposing aeronautical composite materials. A dedicated experiment is thus proposed where accurate test conditions are achieved, inhomogeneous heating is applied, non-intrusive transient measurements are performed and fire dynamics discrepancies are prevented. The

material thermal response is correlated with micrographic imaging carried out post-decomposition to investigate how and why delamination damage occurs and grows.

2. Materials and methods

2.1. Material

The investigation deals with a material used in the aeronautical industry for primary and secondary aircraft structures. The T700GC/M21 is a composite laminate consisting of TORAY T700GC carbon fibres and HEXCEL M21 epoxy resin reinforced by thermoplastic nodules. Sixteen 260 μm -thick M21/35%/268/T700GC unidirectional 268 g.m^2 prepreg plies are stacked and cured to manufacture the composite laminate. This high fibre mass fraction is the consequence of the stacking of two fibre tows in each prepreg tape. The M21 resin is a tough epoxy matrix and exhibits excellent damage tolerance, especially in the case of high energy impacts. To obtain such properties, it contains the thermoplastic nodules around each fibre tow with a characteristic length of 25 μm (Fig. 1). The fibres average diameter is 7 μm and the volume fraction of fibres is 0.57 for the cured material. A 16 ply quasi-isotropic laminate with a final material thickness of 4.16 mm has been studied with the following stacking sequence $[0/45/90/-45/0/45/90/-45]_s$.

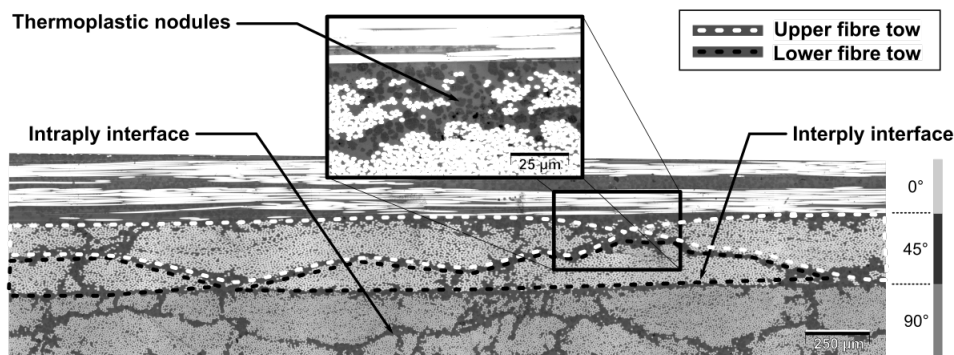


Figure 1. Micrography of the virgin material. T700GC/M21 intra and interply interfaces clearly visible due to the presence of thermoplastic nodules and to the stacking of two fibre tows within each ply.

2.1. BLADE facility

The BLADE facility (characterisation and decomposition laser facility from the French "Banc Laser de cAractérisation et de DEgradation") is devoted firstly to the characterisation of thermo-physical properties of anisotropic materials and secondly to the analysis of the thermal response when they decompose. Even if the apparatus is original, its principle is very simple (Fig. 2).

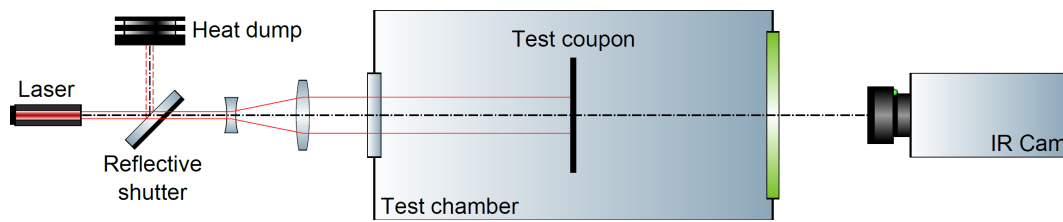


Figure 2. Principle of the BLADE facility.

The apparatus offers two main advantages. First, the enclosure is air-filled, temperature-regulated and the pressure within is decreased down to 3 mBar which is low enough to avoid any convective heat transfer. This last feature makes the BLADE facility original and it results in accurate control of test conditions. Indeed, the determination of the convective heat transfer coefficient would have been very difficult even in a simple geometrical configuration without any guarantee of a good representativity of the convective heat transfer within the chamber. The second advantage of the BLADE facility consists in using a laser instead of a flame to heat up a square-shaped, 80 mm-wide, test coupon during the experiment. The heat flux magnitude and distribution on the material exposed surface may be very difficult to assess accurately and reliably when using standard flames generated by a burner. Instead, the laser provides a heat source, stable in space and time, and it is characterized experimentally preliminary to the tests using inverse heat conduction method on a pure titanium reference material. The Gaussian distribution of the beam collimated at $\varnothing = 21.8 \text{ mm}$ at $1/e^2$ creates a non-uniform heating on the exposed surface which helps revealing the anisotropic behaviour of such composite laminates and offers ultimately valuable data for multi-dimensional models validation. The transient temperature at the back (unheated) side of the test coupon is measured using an infrared thermography camera from the test coupon at rest, then during the heating phase up to the cooling phase when the shutter closes its diaphragm and the laser is switched off.

3. Results and damage analysis

3.1 Thermal behaviour of decomposing laminates

The IR thermography measurements performed on the T700GC/M21 QI test coupons subjected to identical conditions are presented in Fig. 2. The instantaneous temperature maps extracted for each test at $t = 150 \text{ s}$ are presented on the left hand side of Fig. 3. Temperature evolutions as a function of time are also extracted along a horizontal mid-height profile at different locations from the centre and plotted on the right hand side Fig. 3.

A gradual temperature rise of more than 250 K from room temperature is measured on the back surface. The thermal response remains axisymmetric during this first phase and the highest temperature magnitude is observed at the centre of the coupons where the thermal loading at the front side is the highest. Repeatability is evaluated from these 3 tests performed on 3 different coupons and all of them show similar thermal behaviour in the first part of the experiment up to $t = 150 \text{ s}$ (Figs. 34). No in-plane deformation is detected from the IR measurements considering the camera spatial resolution.

The behaviour of the unexposed surface resulting from axisymmetrical Gaussian laser heating on the front surface can thus be addressed under a thermal loading high enough to cause chemical decomposition. The repeatable temperature rise observed in the first part of the experiment is governed by the energy balance between the incoming laser flux, heat conduction within the condensed phase and radiative exchanges with the temperature-regulated chamber walls. Then, temperature-activated

chemical reactions occur and affect the resin through a pyrolysis charring process and probably also affect the new-formed char phase through an oxidation process due to the high temperature magnitude expected on the front face of the material. The temperature maps up to $t = 150$ s (Fig. 3) show that the thermal response of the QI laminates to an axisymmetrical centred thermal loading remains isotropic in the composite panel plane. It is important to note that no ignition is observed all along the experimental process.

After $t = 150$ s, the three coupons present for different time, sudden drops of temperature. These temperature drops are not observed for from the centre of the plate. These drops are the consequence of cracks apparition in the thickness of the laminate and their influence on the thermal response on the opposite face could be linked with the size of these defaults (less than 50 mm wide).

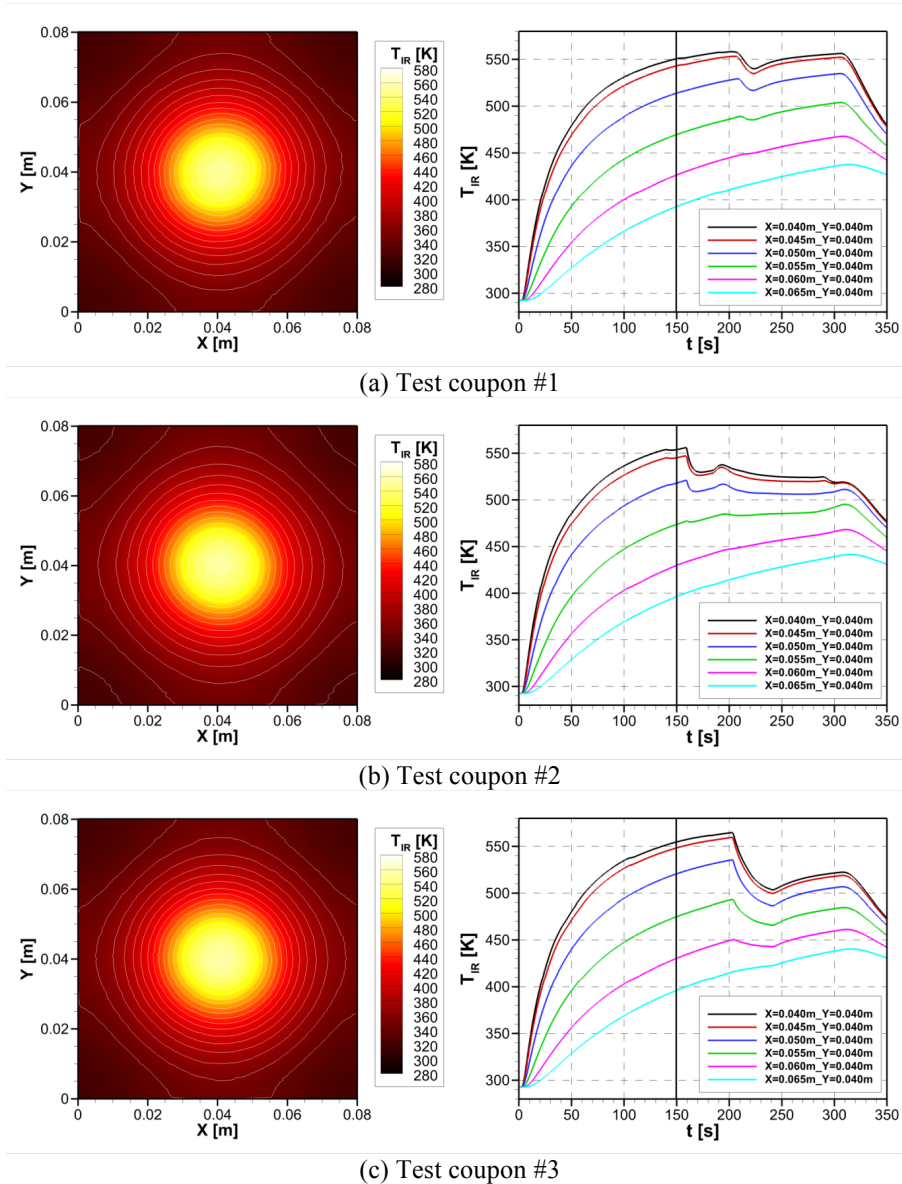


Figure 3. Thermal response on the unexposed surface measured by infrared thermography. Left: instantaneous temperature maps at $t = 150$ s. Right: temperature extracted over time at different locations from the centre of the coupon.

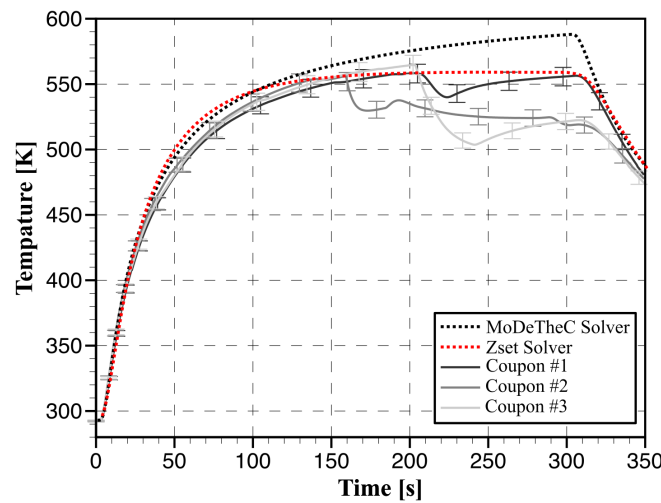
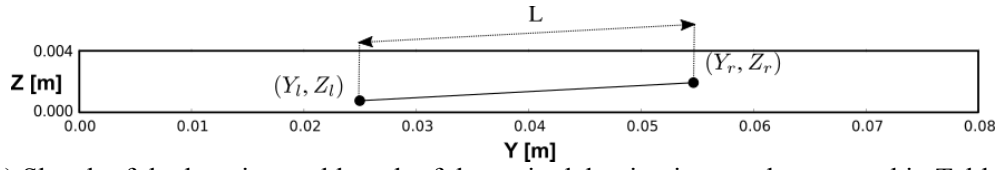


Figure 4. Comparison between experimental results and numerical ones for the evolution of the temperature on the centre of the face opposite to the laser impacted face.

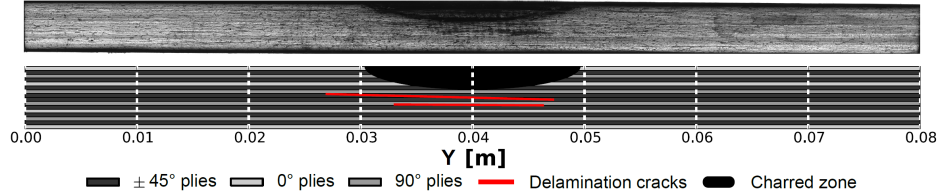
3.2 Post mortem analysis

In order to validate the hypotheses made for the thermal analysis, post-decomposition micrographic analysis is carried out after each test. The micrographs are obtained from longitudinal cross sections of the coupons. A diamond saw device is used and the observed edges are polished from coarse to fine grain polishing paper in order to obtain a mirror finish. Olympus microscope with three axes controller and a monochromatic digital camera (Sensicam PCO) are used to capture the 205 pictures required to observe a whole cross section. The total image reconstruction of the polished edges presented hereafter is performed with an in-house code. Longitudinal median cross-sectional views are presented for each coupon in fig. 5 in order to observe the post-test material condition. Similar observations are taken from transversal median cross sections and are not presented in this paper. For each coupon, the position of the charred zone (in black) and the major delamination cracks (red lines) are reported in a sketch representing the stacking sequence and the damage patterns. The charred zone is idealised by the shape of half an ellipse and the delamination cracks by straight lines. The absolute position of the crack tips for each major delamination crack is reported in Table 1. It is essential to note that only major delamination cracks are reported, although several matrix cracks are present around the charred zone and most of them are under this zone.

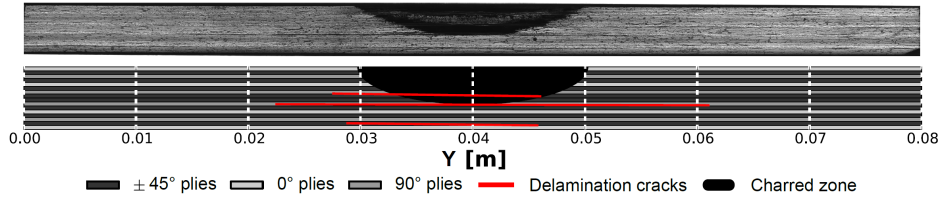
Thanks to these micrographs, several comments could be made. First of all, all coupons present delamination cracks, however, the number, their positions and their size are different for the 3 coupons. The number and the size of delamination cracks are correlated with the number and the depth of the observed temperature drops on the thermal response of the opposite face to the thermal loading (Fig. 4). For example, the biggest temperature drop is observed for the coupon #3 and its correlated with the biggest delamination crack noticed between the first plies of the laminate #3 (close to the opposite face to the thermal loading). On the opposite, the coupon #2, which presents several temperature drops, have three major matrix delamination cracks. Concerning, the charred zone, the depth and the wide of this zone are quite similar, nevertheless, we can observed for the coupon #2 that its depth one is bigger than the two others. The reason of this difference seems to be due to the apparition of a wide delamination crack in the middle of the laminate thickness. The delamination crack reduces the heat transfer in the through-thickness direction and acts as a thermal barrier, which protects the back surface from thermal decomposition. As a consequence, the earlier the delamination crack occurs, the thicker the charred area is because the front part keeps on decomposing while the back part remains temporarily isolated.



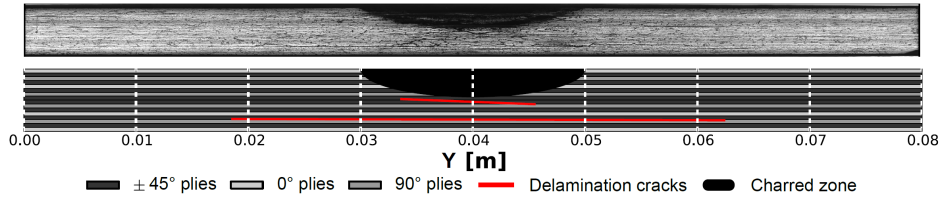
(a) Sketch of the location and length of the main delamination cracks reported in Table 1



(b) Coupon #1



(c) Coupon #2



(d) Coupon #3

Figure 5. Micrographs of the 3 coupons longitudinal cross sections associated with sketches of the major delamination cracks and charred zone for the different specimens.

Table 1. Location and length of the main delamination cracks for coupons #1–3 measured from micrographic images presented in Fig. 5

Coupon	Y_l [m]	Y_r [m]	Z_l [m]	Z_r [m]	L [m]
1	-13.03×10^{-3}	7.19×10^{-3}	1.85×10^{-3}	2.22×10^{-3}	20.22×10^{-3}
1	-6.95×10^{-3}	6.28×10^{-3}	2.54×10^{-3}	2.60×10^{-3}	13.23×10^{-3}
2	-17.51×10^{-3}	20.99×10^{-3}	2.49×10^{-3}	2.56×10^{-3}	38.49×10^{-3}
2	-11.16×10^{-3}	5.75×10^{-3}	3.75×10^{-3}	3.89×10^{-3}	16.91×10^{-3}
2	-12.43×10^{-3}	6.00×10^{-3}	1.78×10^{-3}	1.96×10^{-3}	18.42×10^{-3}
3	-21.42×10^{-3}	22.39×10^{-3}	3.34×10^{-3}	3.43×10^{-3}	43.81×10^{-3}
3	-6.37×10^{-3}	5.49×10^{-3}	2.01×10^{-3}	2.35×10^{-3}	11.87×10^{-3}

The delamination cracks experienced by composite laminates can be associated with both thermal and mechanical loadings. Thermally induced damage concerns the chemical decomposition of matrix and

fibres, the char formation associated with gas production as well. Those phenomena are mainly responsible for the onset of diffuse delamination observed in the experiments. Indeed, the gas pores, resulting from the thermo-chemical decomposition of the matrix that occurs first as the temperature increases, facilitate the onset of microscopic cracks within the condensed phase. This material presents very large resin-rich regions at ply interfaces but also within each ply as illustrated in Fig 1 due to the presence of these thermoplastic nodules. These resin-rich regions offer preferential paths for the cracks initiation and propagation. Fig 6 focuses on two examples of significant delamination cracks for coupon #2 (second and third major delamination cracks of coupon #2 in Table 1). The first delamination crack (in the red box) is located near the charred zone, at the intraply interface of the internal 90° ply. The matrix cracks are highlighted in yellow and can be observed on the right of the delamination crack tip, with very small matrix damage in the intraply interface of the same ply. A higher magnification examination of these small matrix cracks reveals charred thermoplastic nodules (in black in the yellow box). These observations support the assumption of thermally-induced delamination because the matrix reacts first to a temperature rise to create a solid residue (char) and gas pores acting as delamination precursors. Only the matrix (resin and thermoplastic nodules) pyrolysis is characterised by a noticeable mass loss in the thermo-gravimetric analysis performed on this material. These micrographs show that matrix decomposition starts with nodule decomposition. Moreover, they reveal that matrix decomposition can start far from the charred zone, due to elevated temperature.

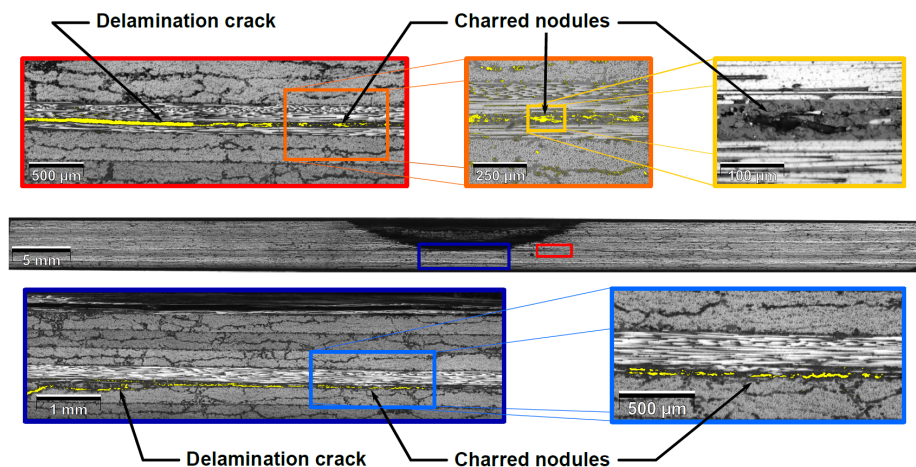


Figure 6. Influence of the charred nodules on the onset of a delamination crack (longitudinal cross section of coupon #2).

In order to validate these assumptions, the model proposed by Biasi and implemented in the MoDeTheC solver (Finite Volume code) [3], has been implemented in the Finite Element code Zebulon. This implementation doesn't take into account the advection equations of the pyrolysis gases and only the thermal degradations of the pyrolysis of the matrix, the char and the fibres oxidation are considered by 3 Arrhenius laws. The Fig 4 presents the comparison between the simulations (MoDeTheC 2D axisymmetric approach, Zset 3D approach) and the 3 coupons presented previously. The thermal responses simulated are very similar and ensure the good estimation of the material thermal degradation before the delamination crack onset. The Fig 7 presents the comparison between the Finite Element code results for the evaluation of the charred zone and the coupon #1 micrograph and demonstrates a very good agreement between experimental data and numerical ones even if the advection of the gases has been neglected. The criterion proposed by Mourritz et al. [2] has been used for estimate the visible char formation and imposes that the mass fraction of the polymer matrix is reduced by $\sim 20\%$, due to decomposition and vaporisation. In the Biasi's model [3], this state corresponds to a value of 0.2 for the pyrolysis reaction growth (α_{Pyro}). Moreover, these numerical

results validate the assumption of thermal degradation “far” from the charred zone and the coupling between thermal degradation and mechanical loading for the onset of delamination cracks in the laminate. The implementation of the Biasi’s model in a finite element code will permit in future work to estimate, by thermo-mechanical analysis, the stresses at the interface, to simulate the damage evolution and the thermal response of the material and to predict the residual strength of the laminate with the objective to design structural part.

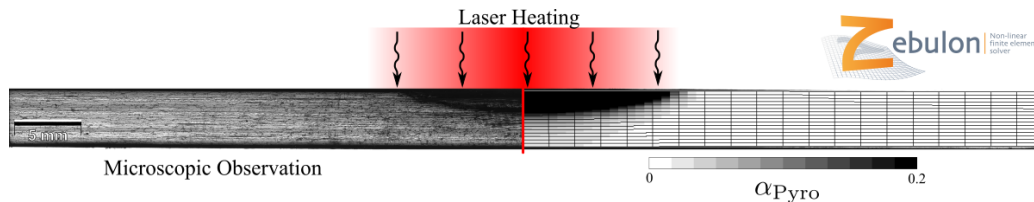


Figure 7. Comparison between experimental (coupon #1 on left) and numerical estimation (on the right) of the charred zone.

3. Conclusions

The current study is based upon the analysis of the composite thermal response subjected to laser-driven heating within a test chamber. As a direct consequence, both experimental surrounding conditions and the heat source supplying the thermal loading distribution into the material exposed surface are accurately controlled and provide a relevant framework for understanding the material behaviour and for developing and validating representative models. The analysis of the transient thermal response with the support of the unsteady numerical simulation and valuable micrographic imaging performed post-decomposition has revealed that heat transfer from the exposed face makes the temperature of the condensed phase increase highly enough to cause pyrolysis of the matrix into a significant depth of the laminate. The orthotropic heat transfer induced by the fibre orientation and the stacking sequence, associated with the inhomogeneous distribution of the heat flux has helped in identifying the physical mechanisms linking thermal decomposition to delamination cracks onset and growth. Future work will focus on the estimation of the internal stress due to the material degradation and the thermal loading in order to estimate the damage scenario. Moreover, a coupling approach between the thermal solver and a thermo mechanical one will permit to estimate the influence of the matrix cracking on

Acknowledgments

This work is funded by ONERA within the frame of an internal collaborative project named MADMAX (French acronym for “Modèles Aérothermomécaniques de Dégradation de MATériaux complexes”) dedicated to the development of aerothermomechanical models for decomposing complex materials.

References

- [1] A.P. Mouritz and A.G. Gibson. *Fire properties of polymer composite materials*. Springer, 2006.
- [2] A.P. Mouritz, S. Feih, E. Kandare, Z. Mathys, A.G. Gibson, P.E. Des Jardin, S.W. Case, and B.Y. Lattimer. Review of fire structural modelling of polymer composites. *Composites Part A: Applied Science and Manufacturing*, 40(12):1800 – 1814, 2009.

[3] V. Biasi, Modélisation Thermique de la Dégradation d'un Matériau Composite Soumis au Feu
PhD thesis of Toulouse University, 2014